IRRADIATION SWELLING, CREEP, AND STRESS ANALYSIS OF LWR FUEL ELEMENTS, COMPUTER CODE ISUNE-2

B.M. MA

Department of Chemical Engineering and Nuclear Engineering, Engineering Research Institute, Iowa State University, Ames, Iowa 50010, U.S.A.

SUMMARY

The irradiation swelling, creep, and stress analysis of light water reactor (LWR) oxide (UO_2) fuel elements is analyzed. The analysis is based on the basic physical and mathematical assumptions and the experimental data of the fuel and cladding (or canning) materials. In the analysis, the nuclear, physical, metallurgical, and thermo-mechanical properties of the fuel and cladding materials under irradiation environment will be examined carefully.

The objectives of the paper are mainly (1) to formulate and carry out the irradiation swelling, irradiation creep, and stress analysis of fuel element for LWR power reactors and (2) to develop a computer code which will facilitate the computations for fuel element design, safety analysis, and economic optimization of the power reactors.

In a general procedure of the analysis, the irradiation swelling, irradiation creep, heat generation, temperature distribution, etc., in the fuel and cladding of the oxide fuel elements during the reactor in operation will be studied. Some theoretical models and relations (on the basis of accepted experimental data) for irradiation swelling and creep in the fuel and cladding materials will be postulated and developed. Some analytical and empirical relations (based on test results) for heat generation and temperature distribution in the fuel elements during fuel restructuring will be derived. The fuel restructure is, in general, divided into the central void, columnar grain, equiaxed grain, and unaffected grain zones (or regions) after a sufficiently long period for the fuel elements to be irradiated (or operated). From these relations derived for irradiation swelling, irradiation creep, heat generation, and temperature distribution in the fuel and cladding, together with the well-known strain-stress, incompressibility, compatibility, and stress equilibrium equations, the irradiation swelling, creep, and stress analysis for the LWR fuel elements can be carried out.

From the analytical results obtained, a computer code, designated as ISUNE-2 (which is in the sequence of Computer Code ISUNE-1 and -1A developed and used previously for liquid-metal fast breeder reactor fuel element design, and safety and economic analysis), can be developed. With some reliable experimental data (measured during fuel elements in operation) as input, the computer code may predict various cases of LWR (oxide or carbide) fuel elements in operation.

The general scope and resulting contribution of this paper is to provide a realistic analysis and a reliable operating LWR fuel element code for use by nuclear power utilities to predict the fuel element behavior in power reactors. The fuel element design, safety analysis, and economic optimization depend largely on the fuel element behavior in the power reactors.

The irradiation swelling, creep, and stress analysis of light water reactor (LWR) oxide (UO_2) fuel elements is analyzed. The analysis is based on the basic physical and mathematical assumptions and the experimental data of the fuel and cladding (or canning) materials. In the analysis, the nuclear, physical, metallurgical, and thermo-mechanical properties of the fuel and cladding materials under irradiation environment are examined carefully.

The objectives of the paper are mainly (1) to formulate and carry out the irradiation swelling, irradiation creep, and stress analysis of fuel elements for LWR power reactors and (2) to develop a computer code which will facilitate the computations for fuel element design, safety analysis, and economic optimization of the power reactors.

In a general procedure of the analysis, the irradiation swelling, irradiation creep, temperature distribution, etc., in the fuel and cladding of the oxide fuel elements during the reactor in operation are studied. Some theoretical models and empirical relations (on the basis of accepted experimental data) for irradiation swelling and creep in the fuel and irradiation creep in cladding materials are postulated and developed. Some analytical and empirical relations (based on test results) for heat generation and temperature distribution in the fuel during fuel restructuring are derived. The fuel restructure is, in general, divided into the central void, columnar grain, equiaxed grain, and unaffected grain zones (or regions) after a sufficiently long period for the fuel elements to be irradiated (or operated). From these relations derived for irradiation swelling, irradiation creep, and temperature distribution in the fuel and cladding, together with the well known strain-stress, incompressibility, compatibility, and stress equilibrium equations, the irradiation swelling, creep, and stress analysis for the LWR fuel elements can be carried out.

From the analytical results obtained, a computer code, designated as ISUNE-2 (which is in the sequence of Computer Code ISUNE-1 and -1A developed and used previously for liquid-metal fast breeder reactor fuel element design, and safety and economic analysis), can be developed. With some reliable experimental data (measured during fuel elements in operation) as input, the computer code may predict various cases of LWR (oxide or carbide) fuel elements in operation.

The general scope and resulting contribution of this paper is to provide a realistic analysis and a reliable operating LWR fuel element code for use by nuclear power utilities to predict the fuel element behavior in power reactors. The fuel element design, safety analysis, and economic optimization depend largely on the fuel element behavior in the power reactors.

1. Introduction

To predict the time-dependent nuclear, physical, metallurgical, and thermo-mechanical properties of reactor fuel elements (or rods) under neutron irradiation conditions, a number of computer codes or programs for computing the performance of oxide fuel elements (or rods) have recently been developed [1-11]. These computer codes can be utilized to facilitate the fuel element design and analysis for light water reactors (LWR's) and liquid-metal fast breeder reactors (LMFBR's), respectively. The physical and mathematical assumptions in each computer code, however, differ (more or less) from one another.

In previous papers [1-4] the thermal, radiation and mechanical analysis for oxide fuel elements of LMFBR's (formulation of Computer Codes ISUNE-1 and -1A) was presented. In this paper the irradiation swelling, irradiation creep, and stress analysis of LWR oxide fuel elements (formulation of Computer Code ISUNE-2) is introduced. In all the papers, the physical and mathematic assumptions are based on fundamental principles and experimental results. The formulation of the computer programs is well defined and rational, and the frequency of convergence of the codes is within reasonable cycles.

The objectives of the paper are to (a) formulate and carry out the temperature distribution, irradiation swelling, irradiation creep, and stress analysis of cylindrical oxide fuel elements, and (b) develop a computer code to predict the fuel element performance of LWR nuclear power plants.

2. Temperature Distribution and Heat Generation

The temperature distribution in the middle cross section of the long, cylindrical LWR fuel element and the heat generation in the fuel zone during a constant linear power operation are analyzed. The analysis begins from the outer surface of the clad and proceeds through the cladding material, the clad-fuel gap, and the outer fuel surface to the central void of the fuel.

2.1 Temperature Distribution in Cladding

In a LWR the heat transfer coefficient, h, between the coolant and the cladding for turbulent flow under forced heat convection in a long tube is represented by the empirical relation

$$N_{Nu} = 0.023(N_{Re})^{4/5}(N_{Pr})^{1/3} \tag{2.1}$$

where $N_{Nu} = hD/K_{co}$, the Nusselt number; $N_{Re} = \rho vD/\mu$, the Reynolds number; $N_{Pr} = C_p\mu/K_{co}$, the Prandtl number; D is diameter or characteristic length of coolant passage; K_{co} is thermal conductivity of coolant; v is coolant velocity, or velocity; ρ is coolant density or density; μ is coolant viscosity; and C_p is specific heat of coolant at constant pressure.

For a given bulk (or designed) coolant temperature T_{co}, the outer surface temperature T_o, the temperature distribution T(r), and the inner surface temperature T_i, of the clad can be calculated from the basic heat transfer equations:

$$T_o = T_{co} + \frac{q}{2\pi r_o h} \tag{2.2}$$

$$T(r) = T_o + \frac{q}{2\pi K_c} \ln(r_o/r) \qquad r_i \le r \le r_o \tag{2.3}$$

$$T_i = T_o + \frac{q}{2\pi K_c} \ln(r_o/r_i) \tag{2.4}$$

in which q is linear power (or heat) rating, K_c is thermal conductivity of cladding material, and r_i, r_o are inner and outer radii of clad.

2.2 Gap Conductance and Temperature Distribution in Bonding Gap

The heat transfer from the outer surface of the fuel to the inner surface of the clad must pass through a bonding gap between the fuel and the clad. The main functions of the bonding gap are to (a) increase the heat conduction from the fuel to the clad, and (b) provide free space for thermal expansion and irradiation swelling of the fuel and cladding materials.

During the fuel elements in normal operation, thermal expansion and irradiation swelling of the fuel and clad materials can cause closure of the bonding gap. Furthermore, thermal-cycling growth and thermal cracking of the oxide fuel can result in local, partial metal interference between the fuel and the clad. The change in the thickness from initial gap to closed gap is to affect the gap conductance (or heat transfer coefficient) of the fuel element. In other words, the heat transferred from the fuel through the gap and the clad to the coolant is to be affected by the gap thickness, L_g, and the gap conductance, h_{gap}.

Experiments have shown that a partial or complete gap closure occurs early in the operating lifetime of the fuel elements [12-14]. Some observations have also indicated that the gap may reopen after it has been closed [15]. Over a sufficiently long time of operation, the irradiation swelling and thermal expansion of the fuel and cladding materials and the cracks formed in the fuel pellets may close the gap again. Figure 1 shows the residual expansion (pellet expansion/pellet diameter) varying with gap thickness (gap thickness/pellet diameter) at various linear power (or heat) ratings from experimental data [12-13] and calculated results. Figure 2 gives some experimental data for gap closure varying with fuel burnup at various linear power ratings [16,17].

After a sufficient burnup of the fuel, volatile impurities and fission gases are to release to the gap through fuel cracks. The primary source of the volatile gases is the sintering atmosphere and impurities in the fuel. The chief sources of fission gases which induce irradiation swelling are the fission yields of Kr^{85} and Xe^{133}. He^4 is a common filling gas for the bonding gap.

2.2.1 Gap Closure

The gap conductance h_{gap} (which may consist of the surface constriction conductance h_s, the gas conductance h_{gas}, and the radiant heat conductance h_r), in the case of gap closure, may be expressed as [7,16-18]

$$h_{gap} = h_s + h_{gas} + h_r = \frac{K_m P_{int}}{aH} + \frac{K_{gas}}{a_1(\delta_f + \delta_c) + (\xi_f + \xi_c)} + h_r \tag{2.5}$$

where $K_m = 2K_cK_f/(K_c + K_f)$, harmonic mean of the fuel and clad thermal conductivities; K_c is thermal conductivity of cladding material as defined; $K = K_f$ is thermal conductivity of fuel material, K_{gas} is thermal conductivity of volatile, fission, and filling gases of the gap; P_{int} is interfacial contact pressure between fuel and clad; a is radius of contact spots with $\delta = 2^{-1/2}(\delta_f^2 + \delta_c^2)^{1/2}$, δ_f and δ_c are arithmetic mean roughness heights of fuel and clad; H is hardness of the clad [16]; ξ_f, ξ_c = temperature jump distances at inner clad and outer fuel surfaces; and h_r = radiant heat transfer conductance (or coefficient). The radiant heat transfer conductance is determined from the radiant heat flux relation, from the fuel and the Stefan-Boltzmann equation

$$h_r = \sigma_{SB}\left[\frac{1}{e_f} + \frac{A_f}{A_c}\left(\frac{1}{e_c} - 1\right)\right]^{-1}(T_f + T_c)(T_f^2 + T_c^2) \tag{2.6}$$

In case the gap is closed or the fuel and clad are in contact, and the fuel surface A_f is practically equal to the clad surface A_c; therefore, eq. (2.6) reduces to

$$h_r = \sigma_{SB}\left[\frac{1}{e_f} + \frac{1}{e_c} - 1\right]^{-1}(T_f + T_c)(T_f^2 + T_c^2) \tag{2.7}$$

where σ_{SB} is the Stefan-Boltzmann constant, e_f, e_c are emissivities of the outer fuel and inner clad surfaces, and $T_f = T_s$, $T_c = T_i$ are as defined. The values of the roughness heights $\delta_f + \delta_c$ and the temperature jump distance $\xi_f + \xi_c$ can be determined experimentally from the relationship between the gas conductivity K_{gas} and gas conductance h_{gas}, eq. (2.5)

$$K_{gas}/h_{gas} = a_1(\delta_f + \delta_c) + (\xi_f + \xi_c) \tag{2.8}$$

The values of $\delta_f + \delta_c$ and $\xi_f + \xi_c$ can be found from Fig. 3 by using the experimental data obtained from various sources. Also, from the slope of the curve (Fig. 3) the value of the parameter a_1 can be obtained.

For purposes of comparison, the predicted and measured gap conductance of oxide fuel rods is shown in Fig. 4.

2.2.2 Gap Opening

In the case the gap is not closed by thermal expansion, irradiation swelling, and cracking of the fuel, and the radial gap thickness $L_g \geq a_1(\delta_f + \delta_c)$, the gas conductance reduces to

$$h_{gas} = \frac{K_{gas}}{L_g + (\xi_f + \xi_c)} \tag{2.9}$$

Therefore, by combining eqs. (2.7) and (2.9), the gap conductance without closure ($h_s = 0$) becomes

$$h_{gap} = h_{gas} + h_r = \frac{K_{gas}}{L_g + (\xi_f + \xi_c)} + \sigma_{SB}\left[\frac{1}{e_f} + \frac{1}{e_c} - 1\right]^{-1}(T_f + T_c)(T_f^2 + T_c^2) \tag{2.10}$$

The temperature T_s (= T_f) at the outer surface of the fuel element can be given by [4]

$$T_s = T_i = \frac{q}{2\pi K_{gap}} \ln\left[\frac{r_i(1 + \epsilon_{\theta_i} + \theta_{th_c})}{r_s(1 + \epsilon_{\theta_s} + \epsilon_{th_f} + \epsilon_s)}\right] \tag{2.11}$$

where K_{gap} is gas thermal conductivity, r_s is outer radius of fuel surface, ϵ_{θ_i} is tangential strain of clad at r_i, ϵ_{θ_s} is tangential strain of fuel at r_s, ϵ_{th_c}, ϵ_{th_f} are thermal expansion strains of clad and fuel, and ϵ_s is irradiation swelling strain. The mean temperature T_g may be written as

$$T_g = (T_s + T_i)/2 \tag{2.12}$$

The gap conductivity in eq. (2.11) is expressed as

$$K_{gap} \cong K_{gas} + 4L_g\,\sigma_{SB}\left[\frac{1}{e_f} + \frac{1}{e_c} - 1\right]^{-1} T_g^3 \tag{2.13}$$

The gap thickness can be calculated from the relation

$$L_g = r_i(1 + \epsilon_{\theta_i} + \epsilon_{th_c}) - (1 + \epsilon_{\theta_s} + \epsilon_{th_c} + \epsilon_s) \tag{2.14}$$

Values for T_s, K_{gap}, and L_g are obtained by combining eqs. (2.11), (2.13), and (2.14) through the forthcoming iteration process since the strains ϵ_{θ_i}, ϵ_{θ_s}, ϵ_{th}, and ϵ_s are involved.

2.2.3 Partial Gap Closed and Partial Gap Open

In the case, the gap is partially closed and partially open due to bambooing (or ridging) along the axial direction of the fuel element, the average gap conductance can be evaluated from the equations obtained in case (1) and case (2). In other words, the mean value of the gap conductance is obtained by averaging the values calculated from the equations derived for the cases of gap closure and gap opening, respectively.

The phenomenon of bambooing (or ridging) of the fuel elements can occur during a LWR power plant in operation, as shown in Fig. 5. The gap at the ridge (or node of a bamboo) is closed while the gap in the valley is open along the axial direction of the fuel element.

2.3 Heat Generation and Temperature Distribution in Fuel

Fuel restructuring and redistribution generally occur in the oxide (or ceramic) fuel after a sufficient time of nuclear irradiation. In the fuel restructuring process, four distinct regions can be formed in the fuel: the central void (or center hole), the columnar grain region, the equiaxed grain region, and the unaffected (or sintered) grain region. These regions and the radius of central void r_v, the outer radius of columnar grain region r_1, the outer radius of equiaxed grain region r_2, and the outer radius of unaffected grain region (outer fuel surface) r_s are schematically shown in Fig. 6. The corresponding temperatures at these surfaces are denoted by T_V, T_1, T_2, and T_s, respectively.

The heat generation rate is approximately proportional to the fuel density ρ for a certain enrichment. For a given linear power (or heat) rating q, the volumetric heat generation rate q_v, in the unaffected grain region, equiaxed grain region and columnar grain region are respectively written as

$$q_{v_3} = q/\pi r_s^2, \quad q_{v_2} = q_{v_3}\rho_2/\rho_3, \quad q_{v_1} = q_{v_3}\rho_1/\rho_3 \tag{2.15}$$

where ρ_1, ρ_2, and ρ_3 are known fractions of the theoretical density (TD) of UO_2 in the three respective regions.

In the unsteady state of power reactor operation the linear power rating of the fuel element may vary as a ramp function from the base linear power rating q_0:

$$q = q_0(1 + mt) \tag{2.16}$$

in which m is the reciprocal time parameter (positive or negative) and t is time, as defined.

In general, the fuel thermal conductivity, $K = K_f$, depends mainly on fuel temperature T and density ρ for specified fabrication processes. In an operating temperature range, the fuel density in each region is practically constant. Thus the thermal conductivity in the UO_2 fuel of LWR can be expressed as [4,19]

$$K_f = K(T,\rho) = C_1 + [T(C_2 - C_3\rho)]^{-1} \tag{2.17}$$

where C_1, C_2, C_3 are constants.

From the Fourier equation of heat conduction, the heat transferred per unit volume of the unaffected grain region at any temperature T(r,t) is

$$q_{v_3} r = -2K_3(T,\rho)\frac{\partial T}{\partial r} \tag{2.18}$$

Substituting eq. (2.17) into eq. (2.18) and performing the integration with appropriate limits yield the temperature distribution in the unaffected grain region as

$$q_{v_3} r_s^2(1 - r^2/r_s^2)/4 = C_1(T - T_s) + (C_2 - C_3\rho_3)^{-1}\ln(T/T_s), \; r_2 \le r \le r_s \;\; T_2 \le T \le T_s \tag{2.19}$$

At the outer surface of the equiaxed grain region, $r = r_2$, $T = T_2$, eq. (2.19) becomes

$$q_{v_3} r_s(1 - r_2^2/r_s^2)/4 = C_1(T_2 - T_s) + (C_2 - C_3\rho_3)^{-1}\ln(T_2/T_s) \tag{2.20}$$

The heat conduction in the equiaxed grain region is given by

$$(q_{v_3} - q_{v_2})(r_2^2/2r) + q_{v_2} r/2 = -K_2(T,\rho)\partial T/\partial r \tag{2.21}$$

Introducing eq. (2.17) into eq. (2.21) and integrating yield the temperature distribution in the equiaxed grain region as

$$q_{v_2}(r_2^2/4)\left[1 - (r/r_2)^2 + (1 - q_{v_3}/q_{v_2})\ln(r/r_2)^2\right] = C_1(r - r_2) + (C_2 - C_3\rho_2)^{-1}\ln T/T_2$$

$$\text{for } r_1 \le r \le r_2,\ T_1 \ge T \ge T_2 \tag{2.22}$$

At the outer radius of the columnar grain region, $r = r_1$, and $T = T_1$, eq. (2.22) becomes

$$q_{v_2}(r_2^2/4)\left[1 - (r_1/r_2)^2 + (1 - q_{v_3}/q_{v_2})\ln(r_1/r_2)\right] = C_1(r_1 - r_2)$$

$$+ (C_2 - C_3\rho_2)^{-1}\ln(T_1/T_2) \tag{2.23}$$

Similarly, the heat conduction in the columnar grain region is

$$q_{v_1}(r^2 - r_v^2)/2 = -K_1(T,\rho)\partial T/\partial r \tag{2.24}$$

Upon substitution and integration, it gives

$$q_{v_1}(r_1^2/4)\left[1 - (r/r_1)^2 + (r_v/r_1)^2\ln(r/r_1)^2\right] = C_1(r - r_1) + (C_2 - C_3\rho_1)^{-1}\ln(T/T_1)$$

$$\text{for } r_v \le r \le r_1,\quad T_v \ge T \ge T_1 \tag{2.25}$$

Let the radius of central void $r = r_v$; the temperature distribution in the columnar region then becomes

$$q_{v_1}(r_1^2/4)\left[1 - (r_v/r_1)^2(1 - 2\ln r_v/r_1)\right] = C_1(r_v - r_1) + (C_2 - C_3\rho_1)^{-1}\ln T_v/T_1 \tag{2.26}$$

From the balance of power output before and after formation of the four regions in the fuel zone, a relation to determine the central void radius (or the ratio r_v/r_1) is

$$r_v/r_1 = \left[(r_2/r_1)^2(q_{v_2} - q_{v_3})/q_{v_1} + (q_{v_1} - q_{v_2})/q_{v_1}\right]^{1/2} \tag{2.27}$$

The value of T_s can be obtained from eq. (2.11) for a given value of r_s. The values of r_v/r_1 and T_v/T_1 can be found from eqs. (2.26) and (2.27). Similarly, the values of r_1/r_2, T_1/T_2, r_2/r_s, and T_2/T_s can be determined from eqs. (2.23) and (2.20), respectively. The temperature distribution in the fuel zone is determined from eqs. (2.19), (2.22), and (2.25) which are parabolic in nature.

Since the temperature distribution in fuel is parabolic and their average thermal gradient $(\partial T/\partial r)_{av}$ occurs at $r_s/3$, the threshold temperature for columnar grain formation as well as concomitant central void formation as a function of irradiation time t, can be expressed as

$$r_s/3t = -\left[C_4\exp(-C_5/T)/T^{3/2}\right](\partial T/\partial r)_{av} \tag{2.28}$$

where C_4, C_5 are constants. For given values of r_s, t, and $(\partial T/\partial r)_{av}$, the threshold centerline temperature $T_c\ (= T_v)$ can be calculated from eq. (2.28).

For the equiaxed grain growth, by analyzing the experimental data of grain growth related to the initial grain size D_0 and the grain size D after annealing of irradiation time t, the cubic equation for the best representation of the results is obtained [4]

$$D^3 - D_0^3 = k_o t\exp(-Q/RT) \tag{2.29}$$

where k_o is constant, Q is activation energy for the process of equiaxed grain growth, and R, T have been defined. With the specified value of average, minimum grain size D for the extent of equiaxed grain in the fuel and the known values of D_0, t, Q, k, and R, the temperature T_2 (= T) can be evaluated from eq. (2.29). This relation is also coupled with the temperature distribution equations derived for the fuel.

The temperature distributions in the fuel element vary with irradiation time for two different cases are shown in Figs. 7 and 8. The predicted temperature rise in the early life of the fuel-element operation has been verified by various experimental data.

The comparison of predicted and measured centerline temperatures of the fuel elements is given in Fig. 9. It is seen that the prediction and measurements of the centerline temperatures are in excellent agreement [21,22].

3. Irradiation Swelling and Fission Gas Release

Apart from irradiation growth and thermal-cycling growth, the most significant radiation effects on nuclear fuel and clad affecting the physico-mechanical stability of reactor fuel elements are irradiation swelling and irradiation creep.

In the previous papers [3,4] a general description for the proposed model of irradiation swelling has been made. In this paper only the resulting equations derived from the model of irradiation swelling are given.

3.1 Irradiation Swelling in Fuel

The volumetric increase due to fission solid-solution swelling $(\Delta V/V)_{sld}$ is expressed as

$$(\Delta V/V)_{sld} = C_b \dot{F} t = C_b q_v t / C_1' \qquad (3.1)$$

where C_b is constant volumetric contribution per fission per unit volume, $\dot{F} = q_v/C_1'$ is the fission rate per unit time t per unit volume of the fuel, q_v is volumetric heat generation rate, and C_1' is conversion constant. The total volumetric increase of fission-gas swelling $(\Delta V/V)_{gas}$ due to fission gas bubbles anchored at the grain boundaries $(\Delta V/V)_{sgb}$, gas bubbles at the dislocation $(\Delta V/V)_{sgd}$, and gas bubbles moving in the grains $(\Delta V/V)_{sgm}$ is represented by the relation [3]

$$(\Delta V/V)_{gas} = (\Delta V/V)_{sgb} + (\Delta V/V)_{sgd} + (\Delta V/V)_{sgm} \qquad (3.2)$$

in which

$$(\Delta V/V)_{sgb} = \frac{1}{L} \sum_{i=0}^{x-1} N_{i,n} (\frac{1}{6} \pi d_i^3) \qquad (3.3)$$

$$(\Delta V/V)_{sgd} = \frac{1}{6} \pi (d')^3 N_o \qquad (3.4)$$

$$(\Delta V/V)_{sgm} = \frac{t - t_{cg}}{t_g} (\frac{1}{6} \pi d_{cg}^3 N_o) \qquad (3.5)$$

L is average parallelepiped length of gas bubbles in the direction of thermal gradient, D is average diameter of the grains in the equiaxed grain region, d_i = bubble diameter on the grain boundary, d' is new bubble diameter at the dislocation, t_g is time required for a bubble to travel across the parallelepiped in the grains, t_{cg} is time required for a bubble to attain its critical size to begin moving, d_{cg} is critical diameter of the grown bubble size, n ($\geq$ x) is number of time intervals, $N_{i,n}$ is number of bubbles per unit area at ith collision after xth time intervals, and N_o is the number of bubbles with diameter d per unit volume. For the isotropic case, the swelling strain $\varepsilon_s = (\Delta V/V)/3$.

3.2 Observation of Irradiation Effect in Zirconium Alloys

The cladding material of LWR fuel elements is zirconium alloys: Zircaloy-2 and Zircaloy-4. The behavior of Zircaloy-2 and Zircaloy-4 is very similar except that during high-temperature water corrision Zircaloy-4 absorbs less hydrogen than does Zircaloy-2. The mechanical properties of Zircaloy are slightly affected by increasing neutron irradiation and hydrogen concentration (forming hydrides). Little irradiation swelling, however, has been observed [23]. So far, no voids have been observed in pure zirconium reported from neutron irradiation experiments. Therefore, the irradiation swelling of Zircaloy may be ignored.

3.3 Fission Gas Release

Fission gas release from the oxide fuel consists of two components: (1) that due to grain growth at elevated temperature, (2) that due to gas bubbles migrating away from grain boundaries when micro- and macro-cracks of the fuel take place.

For component (1), the total number of fission-gas atoms m_g released first to the central void due to grain growth can be evaluated from the semi-empirical equation

$$m_g = m_f \pi r_2^2 \dot{F} t \tag{3.6}$$

where $m_f = 0.27$, the average fission-gas atoms produced per unit volume, and $\dot{F}$, r_2, and t are as defined.

For component (2), the total number of fission-gas atoms, m_b, released from the grain boundaries to the central void from bubbles located between the radii r_j and r_{j-1} of the fuel zone can be given by [3,4]

$$m_b = N_t(4\gamma - \sigma_H d_{cb}) \frac{\pi d_{cb}^2}{6kT} \pi (r_j^2 - r_{j-i}^2) \tag{3.7}$$

in which N_t is total number of bubbles migrating away from the grain boundaries per unit volume, γ is surface tension of fuel material, σ_H is hydrostatic pressure in fuel around the bubble, d_{cb} is diameter of collided bubble, and k, T have been defined before. By adding eqs. (3.6) and (3.7) the total fission gases m_T released first to the central void and then to the plenum of the clad are obtained.

4. Irradiation Creep and Cracks

Nuclear radiation can induce the irradiation creep in the fuel and clad of LWR fuel elements during reactor operation. The rate of irradiation creep $\dot{\varepsilon}$ is, in general, much greater than that of thermal creep.

4.1 Irradiation Creep of UO_2 Fuel

Experiments show that the in-reactor creep rate of UO_2 in the low temperature region (below 800-900 °C) is relatively insensitive or moderately dependent on temperature, and is substantially enhanced over the out-of-reactor creep rate. In the high temperature region (above 1100 °C), however, the creep rate is strongly dependent on temperature with an activation energy Q of the order of the out-of-reactor creep. The creep rate enhancement increases with the fission rate of UO_2 fuel in the reactor. For instance, the creep rate $\dot{\varepsilon}$ of UO_2 in-reactor at a fission rate of 1.2 (10^{13}) fissions/cm^3-sec in the stress range 107-284 kg/cm^2 and temperature range 1030-1190 °C is greater than that of out-of-reactor UO_2 by a factor of about four, as shown in Fig. 10 [4].

Based on experimental data and theoretical analysis [5], it is proposed that the irradiation creep strain ε and creep rate $\dot{\varepsilon}$ of UO_2 in-reactor are expressed as

$$\varepsilon = (t\sigma^n/\sigma_o)\exp(-Q/RT) \tag{4.1}$$

$$\dot{\varepsilon} = (\sigma^n/\sigma_o)\exp(-Q/RT) \tag{4.2}$$

where $\sigma = \sigma(\dot{F})$ is creep stress at a steady state of fission rate $\dot{F}$ defined, σ_o is material creep modules, n is material creep number, and Q, R, and T have been defined previously. Equation (4.2) is essentially a power-function creep law for predicting the creep rate of the oxide fuel operated in reactor. Both σ_o and n depend moderately on the fuel structure, density, irradiation time, etc.

The irradiation creep induced in the oxide fuel is a slow process of plastic deformation. Similarly, the irradiation cracking which occurs in the oxide fuel is also a process of plastic deformation. Fuel cracks are commonly observed to occur in the principal planes and associated with the principal stresses. The initiation of crack nucleation and the direction of crack propagation in the case of multiaxial stresses due to nonuniform thermal expansions and thermal-cycling fatigue may be interpreted by the distortion energy theory. On the basis of structural mechanics it is postulated that under the irradiation environment and yield condition of the distortion energy theory the shearing stress nucleates cracks and the maximum principal stress propagates and extends cracks along the plane normal to the principal stress [26], when the principal plastic stresses occur.

The irradiation cracks of the UO_2 fuel may relieve the principal tensile stresses, release the fission gases from the central void to the plenum, and modify the gap conductance. In general, the cracks have little effect on the fuel density.

4.2 Irradiation Creep, Cracks and Thermal Conductivity of Zircaloy

A considerable amount of interest has been given to the irradiation creep rate $\dot{\varepsilon}$ of Zircaloy. A number of irradiation creep rate laws have also been introduced on the basis of various sets of experimental data [27,28]. In this paper the irradiation creep strain and creep rate of Zircaloy clad at irradiation time t are proposed in the relations [26]

$$\varepsilon = \varepsilon_o(1 - e^{-\varphi t/f})e^{\sigma/\sigma_c} + B\sigma\varphi t \tag{4.3}$$

$$\dot{\varepsilon} = \varepsilon_o \frac{\varphi}{F} \exp(\sigma/\sigma_c - \varphi t/F) + B\sigma\varphi \tag{4.4}$$

where φ is neutron flux, F is reference neutron fluence, σ, σ_c are creep stress and reference creep stress, and ε_o, B are dimensional constants. On the right side of eq. (4.4), the first term represents the thermal creep rate, the second term gives irradiation growth, and the last term expresses the correlated irradiation creep rate of σ and φ for prescribed values of ε_o, B, and F.

5. Stress and Strain Analysis

In the stress and strain analysis of long, cylindrical LWR fuel elements (taking the thermal and irradiation effects into account, the same basic assumptions are made [3,4]. From these assumptions the equations of stress equilibrium, strain compatibility, and stress-strain relations at any irradiation time t are given by [3,4]

$$d\sigma_r/dr + (\sigma_r - \sigma_\theta)/r = 0 \qquad (5.1)$$

$$d\epsilon_\theta/dr + (\epsilon_\theta - \epsilon_r)/r = 0 \qquad (5.2)$$

$$\epsilon_r = [\sigma_r - \nu(\sigma_\theta + \sigma_z)]/E + \alpha T + \epsilon_s + \epsilon_c$$

$$\epsilon_\theta = [\sigma_\theta - \nu(\sigma_z + \sigma_r)]/E + \alpha T + \epsilon_s + \epsilon_c \qquad (5.3)$$

$$\epsilon_z = [\sigma_z - \nu(\sigma_r + \sigma_\theta)]/E + \alpha T + \epsilon_s + \epsilon_c$$

where σ_r, σ_θ, σ_z are radial, tangential and axial principal stresses, ϵ_r, ϵ_θ, and ϵ_z are radial, tangential and axial principal strains, ϵ_s and ϵ_c are irradiation swelling and irradiation creep strains, E is elastic or reduced modulus, ν is Poisson's ratio, α is linear thermal expansion coefficient, and r, T have been defined. For the plane strain state, the axial strain variable, $\epsilon_z = 0$. The thermal expansion strain, αT, and irradiation swelling strain, ϵ_s, are combined in a single term of linear resultant thermal and radiation strain

$$\epsilon_R = \alpha T + \epsilon_s = \epsilon_{th} + \epsilon_s \qquad (5.4)$$

The average value of the linear thermal expansion coefficient for UO_2 may be evaluated from the proposed empirical equation on the basis of experimental data collected between 1000 °C and 2200 °C

$$\alpha = 0.75(10^{-9})(T - 625)^2/(T - 25) + 19.76(10^{-8})(T - 625)/(T - 25) + 1.15(10^{-6}) \qquad (5.5)$$

where the values of 25 °C and 625 °C are chosen as room and coolant temperatures, approximately.

In the creep range (or plastic region), the incompressibility equation is applicable

$$\epsilon_{c_r} + \epsilon_{c_\theta} + \epsilon_{c_z} = \epsilon_{c_r} + \epsilon_{c_\theta} = 0 \quad \text{for } \epsilon_z = 0 \qquad (5.6)$$

To simplify the mathematical manipulation, the new variables of average normal stress s and mean strains e and g are defined as

$$s = (\sigma_r + \sigma_\theta + \sigma_z)/3 \qquad (5.7)$$

$$e = (\epsilon_r + \epsilon_\theta + 3\epsilon_R)/3 \qquad (5.8)$$

$$g = (\epsilon_r - \epsilon_\theta - 3\epsilon_R)/3 \qquad (5.9)$$

If ϵ_R, ϵ_{c_r}, ϵ_{c_θ}, and ϵ_{c_z} are known, the values of ϵ_r and ϵ_θ can be expressed as

$$\epsilon_r = 3(e + g + 2\epsilon_r)/2, \qquad \epsilon_\theta = 3(e - g)/2 \qquad (5.10)$$

From the stress-strain relations, eqs. (5.3), the components of the principal stress can be written as

$$\sigma_r = \frac{3E}{2(1+\nu)(1-2\nu)}\, e + \frac{3E}{2(1+\nu)}\, g + \frac{E}{1+\nu}\,(2\epsilon_R - \epsilon_{c_r}) \qquad (5.11a)$$

$$\sigma_\theta = \frac{3E}{2(1+\nu)(1-2\nu)}\, e + \frac{3E}{1+\nu}\, g - \frac{E}{1+\nu}\,(\epsilon_R + \epsilon_{c_\theta}) \qquad (5.11b)$$

$$\sigma_z = \frac{3E}{(1+\nu)(1-2\nu)} e - \frac{E}{1+\nu} (\epsilon_R + \epsilon_{c_z}) \qquad (5.11c)$$

By introducing eq. (5.10) and the first two of eqs. (5.11) into eqs. (5.1) and (5.2), the new equilibrium and compatibility equations in terms of the defined variables e and g can be obtained. With appropriate boundary conditions, e and g can be determined.

For thin clad operated in a moderate temperature range, the material constants (elastic or reduced modulus, Poisson's ratio, linear thermal expansion coefficient, etc.) vary moderately along the clad radius. The average values of E, ν, α, etc. can be used. For the thick fuel zone, the thermal gradients and the density changes due to nuclear irradiation are so large that the average material constants are no longer adequate for use in the fuel zone. Therefore, for a thin clad a closed-form solution can be obtained, but for a thick fuel zone a finite-difference (or finite-element) method must be used to solve the differential equations with temperature material constants.

5.1 Closed-Form Solution of the Clad

Consider the thin clad a hollow cylinder with inner and outer radii r_i, r_o subjected to an internal gas or gap pressure P_g, an external pressure P_o due to coolant, a radial temperature distribution T(r), and an irradiation creep rate $\dot{\epsilon}_c$.

Upon substitution of ϵ_R, ϵ_θ, σ_r, σ_θ from eqs. (5.10), (5.11a), and (5.11b) into eqs. (5.1) and (5.2), the equilibrium and compatibility equations become

$$\frac{1}{1-2\nu}\frac{de}{dr} + \frac{dg}{dr} = -\frac{2(g+\epsilon_R)}{r} - \frac{4}{3}\frac{d\epsilon_R}{dr} + \frac{2}{3}\frac{d\epsilon_{c_r}}{dr} - \frac{2(\epsilon_{c_r} - \epsilon_{c_\theta})}{3r} \qquad (5.12)$$

$$\frac{de}{dr} - \frac{dg}{dr} = \frac{2(g+\epsilon_R)}{r} \qquad (5.13)$$

Solving for e and g from eqs. (5.15) and (5.16) yields

$$e = \frac{1-2\nu}{3(1-\nu)}\left[\epsilon_{c_r} - 2\epsilon_R + \int_{r_i}^{r} \frac{\epsilon_{c_r} - \epsilon_{c_\theta}}{r} dr\right] + A_1 \qquad (5.14)$$

$$g = \frac{2(1+\nu)}{3(1-\nu)}\frac{1}{r^2}\int_{r_i}^{r} r\epsilon_R\, dr + \frac{1-2\nu}{3(1-\nu)}\left[\epsilon_{c_r} - 2\epsilon_R - \frac{1}{r^2}\int_{r_i}^{r} (\epsilon_{c_r} + \epsilon_{c_\theta}) r dr\right] + \frac{A_2}{r^2} \qquad (5.15)$$

where A_1 and A_2 are the integration constants. The boundary conditions for the clad at the inner and outer radii are

$$r = r_i,\ \sigma_r = -P_g; \quad r = r_o,\ \sigma_r = -P_o \qquad (5.16)$$

where the coolant pressure P_o is a given (or designed) value, and the internal gas pressure P_g will be given later. The integrals in eqs. (5.14) and (5.15) can be performed analytically to obtain a closed-form solution. These integrals can also be evaluated by a numerical (or computer) method when the values of integrands at each interval are prescribed.

5.2 Finite-Difference Method of Fuel Zone

The finite-difference method is applied to obtain a solution for the fuel zone. The fuel zone may have an outer surface radius r_s and a central void radius r_v (see Fig. 6) after a sufficient irradiation time (or burnup) has been attained. There are also the fission gas pressure P_v in the central void and gas (or gap) pressure in the fuel-clad gap. The fuel zone is divided into N arbitrary intervals along the radius so that there are N + 1 stations. The first station is taken at the inner radius r_v (or at the center of the fuel element).

In the application of the finite-difference method, the compatibility equation, eq. (5.16), between station i and station i - 1 becomes

$$\frac{e_i - e_{i-1}}{r_i - r_{i-1}} - \frac{g_i - g_{i-1}}{r_i - r_{i-1}} = \frac{g_i + \epsilon_{R_i}}{r_i} + \frac{g_{i-1} + \epsilon_{R_{i-1}}}{r_{i-1}} \tag{5.17}$$

Similarly, the equilibrium equation, eq. (5.15), becomes

$$\begin{aligned} \frac{3E_i}{2(1+\nu_i)}\left[\frac{e_i}{1-2\nu_i} + (1 + \frac{r_i - r_{i-1}}{r_i})g_i\right] &= \frac{3E_{i-1}}{2(1+\nu_{i-1})}\left[\frac{e_{i-1}}{1-2\nu_{i-1}} + (1 - \frac{r_i - r_{i-1}}{r_{i-1}})g_{i-1}\right] \\ &- \frac{E_i}{2(1+\nu_i)}\left[2(\epsilon_{R_i} - \epsilon_{c_{r_i}}) + \frac{r_i - r_{i-1}}{r_i}(3\epsilon_{R_i} - \epsilon_{c_{r_i}} + \epsilon_{c_{\theta_i}})\right] \\ &+ \frac{E_{i-1}}{2(1+\nu_{i-1})}\left[2(2\epsilon_{R_{i-1}} - \epsilon_{c_{r_{i-1}}}) - \frac{r_i - r_{i-1}}{r_{i-1}}(3\epsilon_{R_{i-1}} - \epsilon_{c_{r_{i-1}}} + \epsilon_{c_{\theta_{i-1}}})\right] \end{aligned} \tag{5.18}$$

Similar equations of compatibility and equilibrium can be written between station i - 1 and station i - 2, etc. The combination of eqs. (5.17) and (5.18) gives e and g at the ith station in terms of those at the i - 1 station. The values of e and g at the ith station can also be correlated to those at the first station, etc. After e_1 and g_1 are found, all the other values of the e and g can be obtained.

At the n + 1 station, i.e., the outer surface of the fuel zone (the outer boundary condition), the radial stress of the fuel is equal to the gas or gap pressure

$$\sigma_{r_{N+1}} = -P_g = - \frac{P_{in}(r_i^2 - r_s^2)T_g}{[r^2(1 + \epsilon_{\theta_i} + \epsilon_{th_c})^2 - r_s^2(1 + \epsilon_{\theta_s} + \epsilon_{th_f} + \epsilon_s)^2]T_{in}} \tag{5.19}$$

where P_{in} is initial pressure of gases, T_{in} is initial temperature of gases in the fuel-clad gap, and T_g, r_i, r_s, ϵ_{θ_i}, ϵ_{θ_s}, ϵ_{th}, and ϵ_s have been defined [eqs. (2.11) and (2.12)]. In the case where the gap is closed, the fuel-clad contact pressure might be small or comparable to the gas pressure because the fuel surface becomes soft and rough due to high irradiation temperatures.

At the first station, i.e., at the center of fuel zone (the inner boundary condition), for a solid fuel element the boundary condition is simply $\sigma_{r_1} = \sigma_{\theta_1}$. When σ_{r_1} and σ_{θ_1} are introduced into eqs. (5.11a) and (5.11b), g_1 is found:

$$g_1 = (\epsilon_{c_{r_1}} - \epsilon_{c_{\theta_1}} - 3\epsilon_{R_1}) \tag{5.20}$$

For the fuel element with a central void, the boundary condition at the first station is

$$\sigma_{r_1} = -P_v = -\left[\frac{P_{in}T_v}{T_{in}(1 + \epsilon_{\theta_1} + \epsilon_{th_c})^2} + \frac{(0.27\pi r_s^2 Ft + M_b)kT_v}{\pi r_v^2(1 + \epsilon_{\theta_v} + \epsilon_{th_f} + \epsilon_s)^2}\right] \quad (5.21)$$

where M_b is the total volatile and fission gas atoms releasted from grain boundaries in the unaffected grain region to the central void, and P_v, P_{in}, T_v, F, t, etc., have been defined. The values of e_1 and g_1 can be found from eqs. (5.11a), (5.14), and (5.15) after substitution from eq. (5.21).

In the case where extensive cracks have taken place, the gases of the central void, the fuel-clad gap, and the plenum of the fuel element are interconnected in equilibrium. The two boundary conditions then become identical at the outer and inner surfaces of the fuel zone:

$$\sigma_{r_{N+1}} = \sigma_{r_1} = -P_g = -\frac{M_t R}{V_v/T_v + V_g/T_g + V_p/T_p} \quad (5.22)$$

in which V_v, V_g, V_p are volumes of the central void, gap, and plenum, M_t is total mass (in moles) of gases, T_p is gas temperature in the plenum (slightly higher than coolant temperature T_{co}), and T_v, T_g, R are as previously defined.

Once e's and g's are solved from the equlibrium and compatibility equations in either the closed-form solution or the finite-difference method described above, all principal stresses and strains produced in the mid-plane of the LWR fuel elements can be determined. By such successive or iterative processes, the complex nonlinear problem has been solved in a simple, linear manner.

6. Iteration Method and Computer Code ISUNE 2

The principle of the iteration method is to solve the nonlinear, thermal elastoplastic problem under the condition of heat generation, irradiation swelling, and irradiation creep of LWR fuel elements. The creep (or plastic) strains predicted or presumed at each step involve, practically, the solution of a linear problem.

The procedure to carry out the iteration method is similar to that given before [3,4].

A computer code, ISUNE 2, written in FORTRAN IV language and adapted for the IBM 360 Computer at Iowa State University Computer Center is developed to perform the irradiation swelling, irradiation creep, and stress analysis for LWR fuel elements in unsteady-state fuel restructuring. The fuel is UO_2 or $UO_2 \cdot PuO_2$ for Pu recycling in LWR.

7. Conclusions

From the preceding irradiation swelling, irradiation creep, and stress analysis and the comparisons between the analytic results and the experimental data of the long, cylindrical LWR fuel elements, the following primary conclusions are drawn:

(1) The relationships of the fuel-clad gap thickness and gap conductance for the case of gap closure, gas opening, or partial closure and opening are derived based on experimental data.

(2) From the analytical and experimental creep data, some empirical equations for irradiation creep laws of the fuel and cladding materials are proposed for the fuel-element stress analysis [eqs. (4.1)-(4.4)]. These equations are seemingly on a sound analytical and experimental basis.

(3) The initiation of crack nucleation and the direction of crack propagation in the UO_2 (or ceramic) fuel (due mainly to nonuniform thermal expansion and thermal-cycling fatigue) may be interpreted by the distortion energy theory. It is postulated that under the irradiation environment and yield condition of the distortion energy theory the shearing stress nucleates cracks and the maximum principal stress propagates and extends cracks along the plane normal to the principle stress when the principle plastic or creep stresses occur in the fuel elements.

(4) The formulation and performance of irradiation swelling, irradiation creep, and stress analysis of the LWR fuel elements and the development of a relatively complete computer code, ISUNE 2, will facilitate the computations for the fuel element design, safety analysis, and economic improvement of the nuclear power plants.

Acknowledgments

The author wishes to express his appreciation to the Department of Chemical Engineering and Nuclear Engineering, the College of Engineering, and the Engineering Research Institute at Iowa State University for their encouragement and the support of the research work.

References

[1] CHENG, C. K., MA, B. M., "ISUNE 1 - A Computer Code for Performing Thermal, Radiation, and Mechanical Analysis of Oxide Fuel Elements of Fast Reactor in Unsteady State," Trans. Amer. Nucl. Soc., 12(1), 125 (1970).

[2] MA, B. M., CHENG, C. K., "Computer Code Abstract, ISUNE 1," Nucl. Sci. and Engr., 42, p. 112 (1970).

[3] MA, B. M., "Thermal, Radiation, and Mechanical Analysis for Fast Reactor Fuel Elements," (ISUNE 1A), Proc. First International Conf. on Structural Mechanics in Reactor Technology, Paper No. C4/3, Berlin, West Germany, September 19-24, 1971.

[4] CHENG, C. K., MA, B. M., "Thermal, Radiation and Mechanical Analysis - Fuel Restructuring Unsteady State of Cylindrical Oxide Elements in Fast Reactors," Nucl. Sci. and Engr., 48, pp. 139-158 (1972).

[5] DUNCOMBE, E., FRIEDRICK, C. M., FISCHER, J. K., "CYGRO-3 - A Computer Program to Determine Temperatures, Stresses and Deformations in Oxide Fuel Rods," USAEC Research Report WAPD-TM-961, Westinghouse Electric Corp. (March 1970).

[6] HANN, C. R., PANISKO, F. E., "User's Guide for GAPCON: A Computer Program to Predict Fuel-to-Cladding Heat Transfer Coefficients in Oxide Fuel Pins," (LMFBR), Hanford Engineering Development Laboratory, HEDL-TME-128 (September 1972).

[7] HANN, C. R., BEYER, C. E., PARCHEN, L. J., "GAPCON-THERMAL: A Computer Program for Calculating the Gap Conductance in Oxide Fuel Pins," Battelle Pacific Northwest Laboratories, BNWL-1778 (September 1973).

[8] OLDBERG, S., Jr., "BEHAVE-2: Oxide Fuel Performance Code in Two Spatial Dimensions and Time," USAEC Research Report GEAP-13788, General Electric Co. (September 1972).

[9] JANKUS, V. Z., WEEKS, R. N., "LIFE-1: A FORTRAN IV Computer Code for the Prediction of Fast-Reactor Fuel-Element Behavior," Argonne National Laboratory, ANL-7736 (November 1970).

[10] JANKUS, V. Z., WEEKS, R. N., "LIFE-2: A Computer Analysis of Fast-Reactor Fuel-Element Behavior as a Function of Nuclear Operating History," Intern. Jour. Nucl. Engr. Design, 18, pp. 83-96 (1972).

[11] HOMAN, F. J., et al., "FMODEL: A FORTRAN IV Computer Code to Predict In-Reactor Behavior of LMFBR Fuel Pins," Oak Ridge National Laboratory, ORNL-4825 (January 1973).

[12] BAIN, A. S., "Microscopic Autoradio-graphic and Fuel/Sheath Heat Transfer Studies on UO_2 Fuel Elements," AECL-2588, (June 1966).

[13] JANVIER, J. C., de BERNARDY de SIGOYER, B., DELMES, R., "Irradiation of Uranium Oxide in Strong Cladding - Effect of Initial Diametral Gap on Overall Behavior Program CC-7," CEA-R-3358, (October 1967).

[14] LAWRENCE, L. A., "Power Cycling Effect on Fuel-Cladding Gap Closure," Transactions, Amer. Nucl. Soc., 15(1), 223 (1972).

[15] BELLAMY, R. G., RICH, J. B., "Grain Boundary Gas Release and Swelling in High Burnup Uranium Dioxide," <u>J. Nuclear Materials</u>, 33, pp. 64-76, 1969.

[16] BOESCHOTEN, F., VAN DER HELD, E. F. M., "The Thermal Conductance of Contacts Between Aluminum and Other Metals," <u>Physica</u>, 23, 37-44 (1957).

[17] ROSS, A. M., STOUTE, R. L., "Heat Transfer Coefficients Between UO_2 and Zircaloy-2, AECL-1552 (or CRFD-1075)(June 1962).

[18] LAMING, L. C., "Thermal Conductance of Machined Metal Contacts," <u>Proc. Intern. Heat Transfer Conf.</u>, Part I, 65-76, ASME, New York, August 28-September 1, 1961.

[19] ASAMOTO, R. R., ANSELIN, F. L., CONTI, A. E., "The Effect of Density on the Thermal Conductivity of Uranium Dioxide," <u>J. Nucl. Materials</u>, 29, pp. 67-81 (1969).

[20] NICHOLS, F. A., "Theory of Columnar Grain Growth and Central Void Formation in Oxide Fuel Rods," <u>J. Nucl. Materials</u>, 22, pp. 214-262 (1972).

[21] ASAMOTO, R. R., et al., "Center Temperature Measurements of Mixed Oxide Fuel - Zero to 3,000 MWd/Te," GEAP-13603 (1970).

[22] KJAERHEIM, G., ROLSTAD, E., "In-Pile Determination of UO_2 Thermal Conductivity, Density Effects and Gap Conductance," HRB-80 (1967).

[23] THOMAS, W. B., et al., "Irradiation Experience with Zircaloy-2," <u>Proc. 3rd U.N. Conf. on Peaceful Uses of Atomic Energy</u>, 10, pp. 80-87 (1964).

[24] PERRIN, J. E., "Irradiation-Induced Creep of Uranium Oxide," <u>J. Nucl. Materials</u>, 39, pp. 175-182 (1971).

[25] MA, B. M., "A Creep Analysis of Rotating Solid Disks," <u>J. Franklin Institute</u>, 267, pp. 149-165 (1959).

[26] MA, B. M., "Irradiation Swelling, Creep, Thermal-Shock and Thermal-Cycling Fatigue Analysis of Cylindrical CTR First Wall," <u>Intern. J. Nucl. Engr. Design</u>, 28, pp. 1-30 (1974).

[27] ROSS-ROSS, P. A., HUNT, C. E. L., "The In-Reactor Creep of Cold-Worked Zircaloy-2 and Zircaloy-2.5 wt. percent Niobium Pressure Tubes," <u>J. Nucl. Materials</u>, 26, pp. 2-17 (1968).

[28] NICHOLS, F. A., "Theory of the Creep of Zircaloy During Neutron Irradiation," <u>J. Nucl. Materials</u>, 30, pp. 249-270 (1969).

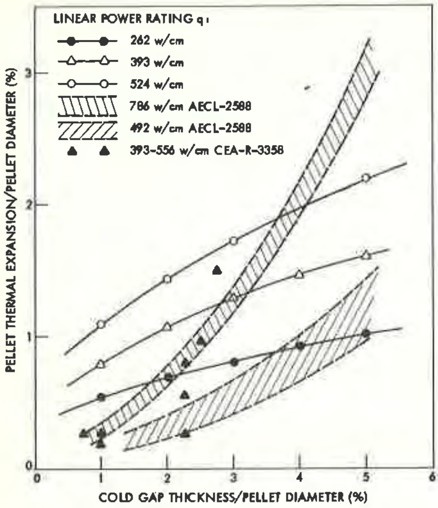

Fig. 1. Pellet thermal expansion varies with cold gap thickness.

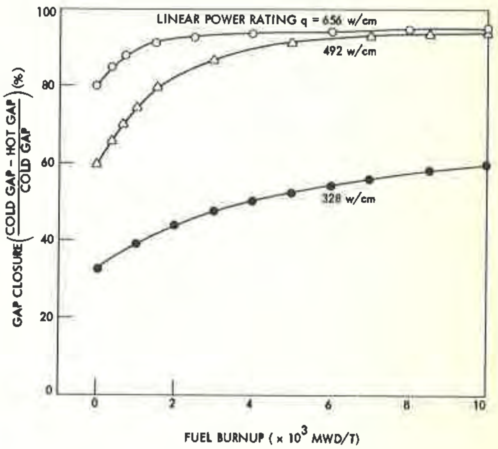

Fig. 2. Calculated gap closure varies with fuel burnup at various linear power ratings.

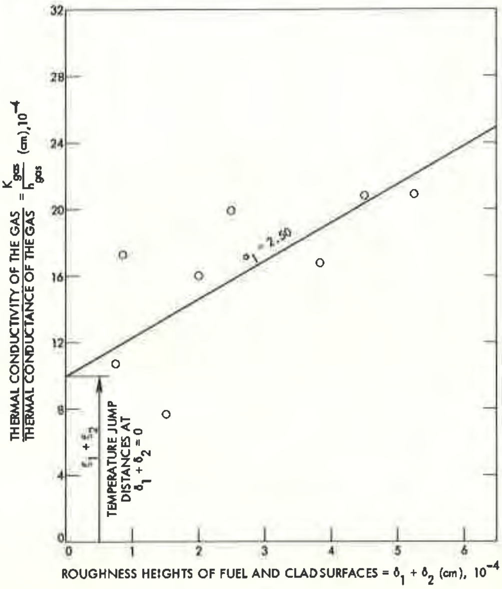

Fig. 3. Graphic determination of the temperature jump distances, surface roughness heights and the parameter a_1.

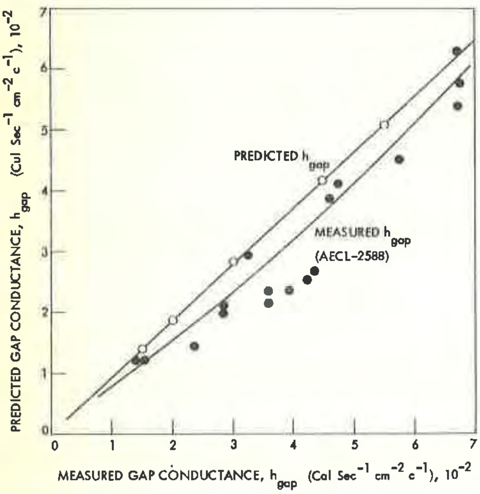

Fig. 4. Comparison of predicted and measured gap conductance of the oxide fuel elements.

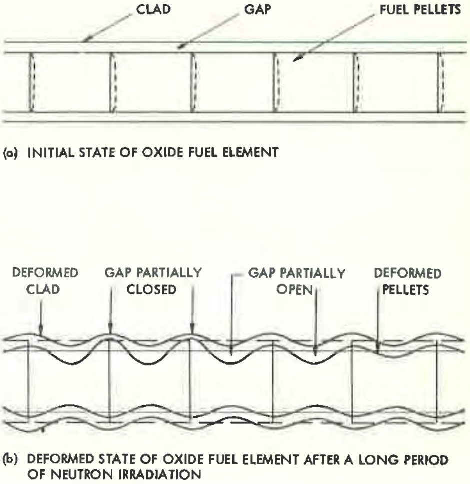

Fig. 5. Bambooing (or ridging) of oxide fuel element after a long period of neutron irradiation.

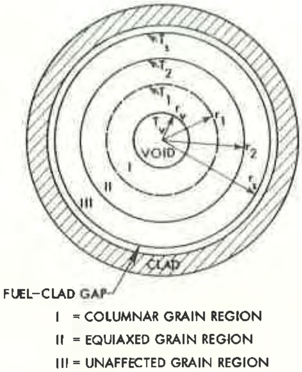

Fig. 6. Typical cross section of an irradiated oxide fuel element.

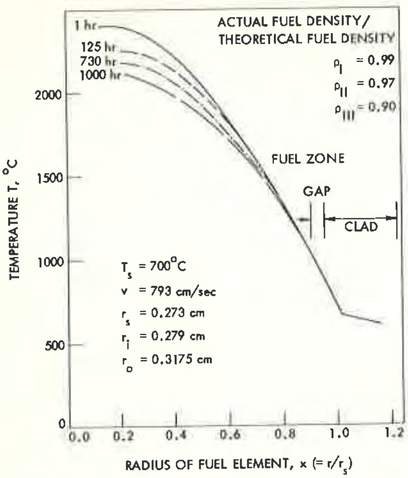

Fig. 7. Temperature distribution in the fuel element varies with irradiation time, linear power rating q = 492 w/cm.

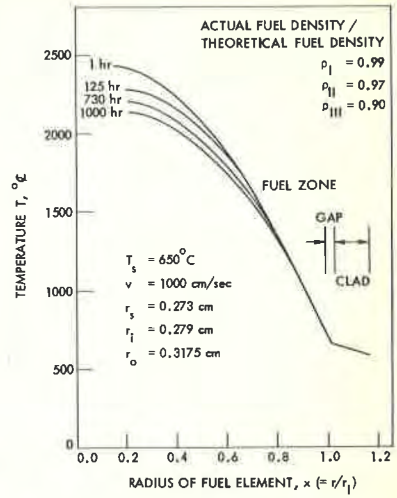

Fig. 8. Temperature distribution in the fuel element varies with irradiation time, linear power rating q = 510 w/cm.

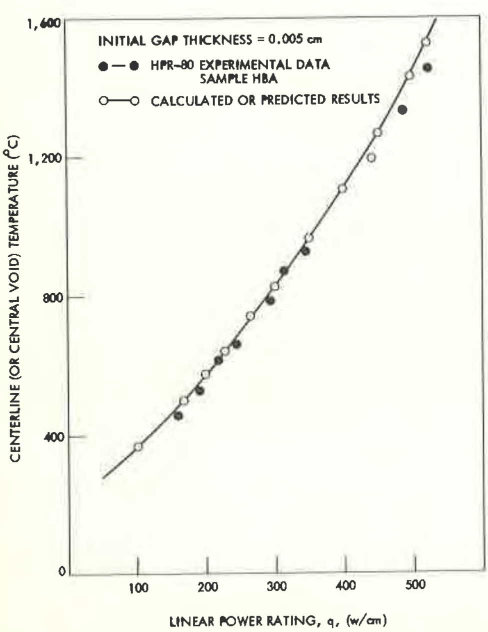

Fig. 9. Comparison of calculated and measured centerline temperature of the oxide fuel element.

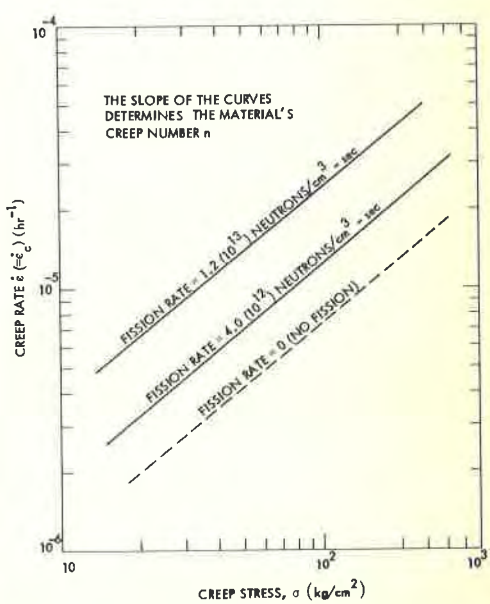

Fig. 10. Creep rate of UO_2 fuel varies with creep stress for different fission rates.